VEÐURSTOFA ÍSLANDS

Report
01003

Ragnar Slunga

Foreshock activity, fault radius and silence – earthquake warnings based on microearthquakes

VÍ-JA03
Reykjavík
February 2001

Report - Greinargerð
01003

Ragnar Slunga

Foreshock activity, fault radius and silence – earthquake warnings based on microearthquakes

VÍ-JA03
Reykjavík
February 2001

CONTENTS

1 INTRODUCTION

The Icelandic microearthquake network has produced more than 150000 microearthquake source mechanisms for microearthquakes larger than M_L=–0.5 since 1991. During June 2000 two major earthquakes occurred within the South Iceland lowland (SIL) with $M_S \geq 6$, the first on June 17 had M_S=6.6. In addition a M_S=5.8 earthquake occurred in June 1998 within the triple junction area west of SIL. This constitutes a valuable database for research on the processes leading to major earthquakes.

From studies in other areas on crustal strike–slip earthquakes it has been found that foreshock activity can often be seen from 5–30 days before the main shock and that this foreshock activity is highest the last 24 hours before the main shock. The foreshock activity is typically within a few kilometers of the mainshock epicenter.

Those studies also have indicated that all earthquakes do not have $M_L \geq 2$ foreshocks. Instead there are several reports that seismic silence has preceded the earthquake.

In addition there are also several reports that the Gutenberg b–value decreases a few months prior to large earthquakes in the area and also that there are indications of a power law increase in seismic activity before large earthquakes.

All these reported observations indicate that the large earthquakes are not coming as complete surprises, the processes leading to a large earthquake may reveal itself by affecting different aspects of the microearthquake activity.

The rate– and state–dependent model of friction on crustal fractures is a new paradigm in earthquake source theories. One of the interesting aspects is that there exists a minimum fault radius for any given earthquake generating fracture and load system. Boatwright and Cocco (1996) pointed out that different parts of the fractures with different minimum fault radius for the earthquakes may be active at different stages of the accelerating process leading to a large earthquake.

Based on these results a number of earthquake warning parameters earthquake warning algorithm has been defined and was tested retrospectively on the SW–Iceland. A paper will be submitted for publication. The following presentation and discussion is based on that paper.

2 THE SOUTH ICELAND SEISMIC ZONE (SISZ)

The South Iceland seismic zone (SISZ) connects two parts of the mid–Atlantic spreading ridges. All large earthquakes so far studied have been on N–S fractures. This was used in defining the geometry of the areas used in computing statistical parameters based on the microearthquake observations.

3 PARAMETER 1 – THE SLIP–WEIGHTED SEISMICITY CONCENTRATION (SWSC)

The estimate of seismicity rate (number of events within a given time and space) can only increase at times of new microearthquakes and the increase will in general be largest close to the new microearthquake. Thus a simplification which is reasonable is to compute the seismicity rate only at times and places of the microearthquakes.

The seismicity concentration was defined as the number of microearthquakes (no magnitude restriction and each weighted with the inverse of the distance from the new mi-

croearthquake) within a time period of 21 days (3 weeks) before the new microearthquake and within a radius of 6 km around its position.

Now, as pointed out above there are several reports of foreshocks and foreshock activity peaking the last 24 hours before the main event. This is the reason for defining the slip–weighted seismicity concentration (SWSC), by multiplying the seismicity concentration by the square root of the slip size of the new microearthquake. The slip size is measured in millimeters. The reason for taking the square root is to reduce the influence of very large slip sizes.

One can note that the idea of relying on the slip U of the last event is in agreement with the view that the major earthquakes are preceded by a phase of accelerating crustal deformations which then is likely to generate microearthquakes with increasing slip sizes.

Note that it also reduces the possibilities for a typical small mainshock ($M_L \leq 2$–3.5) followed by aftershocks to cause high SWSC values as the largest slip sizes normally are in the beginning of such processes.

4 PARAMETER 2 – THE MODIFIED MEDIAN OF THE FAULT RADIUS

As mentioned above the microearthquake fault radius may be a key parameter in monitoring the crustal deformation (fault movements). The author defined the modified median of the fault radius in the following way: For all microearthquakes within a specified area and a specified time interval the 25%, 50%, and 75% values of the fault radius distribution were summed and divided by 3. This estimate of the modified median was again only estimated for times and places of each microearthquake. A time period of 21 days was again used but the areas were chosen as N–S strips with a width of +/–3 km (longitude from the microearthquake) and extending from 63.9°N to 64.1°N (22 km). If the number of events exceeded 80 the time interval was shortened so only the 80 events just before the microearthquake was included when computing the modified median.

The fault radius has statistically a positive correlation to magnitude. Thus an increase in fault radius median is often related to an increase in magnitude median, that means to a lowering of the b–value. However, this is not always so and as the fault radius is more directly related to recent models of fault friction and its consequences we preferred to use the fault radius instead of b–value in this study.

5 PARAMETER 3 – THE "SANDWICH" SEISMICITY RATIO (Q)

The "sandwich" parameter expresses an effort to combine foreshock activity on a fault with the silence around it due to stress reduction during the phase of accelerated slip on the fault. We used the same N–S strips as above and computed at time and place of each microearthquake the number of microearthquakes within 21 days (before the microearthquake) and within such a strip. In addition we also computed the number of events outside this strip but within 10 km west or east of the central line of the strip. Thus the three parts make a "sandwich" pattern. Our "sandwich" seismicity ratio is then the ratio of the number of events within the central strip divided by the number of events within the whole extended strip. Note that the area outside the central strip is $2*7/6 = 2.3$ times larger than the area of the central strip. If all events during the time interval are

within the central strip our ratio Q will equal 1.

6 THE LARGER EARTHQUAKES ($M_L \geq 4.9$)

The following larger events have occurred within the SISZ during the 9 year period we have studied, i.e. from July 1, 1991, to October 25, 2000.

Event	M_L	M_S	*Area*
1997: August 24	4.95	—	Hengill
1998: June 04	5.30	5.8	Hengill
1998: November 13	5.05	—	Hengill
1998: November 14	4.92	—	Hengill
2000: June 17	5.9	6.6	SIL
2000: June 21	5.7	6.4	SIL

7 EXAMPLES OF THE BEHAVIOUR OF OUR THREE PARAMETERS

The modified median of the fault radius, FRMM, was early found to be a good precursor to the Hengill earthquakes. This is shown in Figures 1–5.

Figure 6 shows that this is not so before the largest of our earthquakes, the June 17, 2000, event within the SIL area. However, Figures 6 and 7 show that there is a peak in FRMM about 4 months before the two SIL earthquakes. Note that also before the largest Hengill earthquake (Figure 1), there is a peak about 3–4 months before the event. Note also that although the FRMM shows rather similar overall pattern the peaks 4 months ahead of each of the three major earthquakes are rather dominating. Thus the FRMM highs seem to be an intermediate precursor. Note that this is similar to the b–value lows in several published studies.

From a statistical point of view the short–term behaviour of the FRMM in the Hengill area before the three largest events is more convincing. The short–term behaviour gives, however, support to the indicated intermediate–term prognostic value of the FRMM as it obviously is linked to the earthquake generating processes as predicted by theory.

The third parameter is the "sandwich" seismicity ratio, Q. This is defined as the ratio of the seismicity rate within a central strip and the sum of the seismicity rates within the surrounding strips. This is illustrated in Figure 8 before the large SIL earthquake on June 17. As can be seen there is both an increased activity within the central strip and a silence in the surroundings.

Finally Figures 9–11 show the behaviour of SWSC before the three largest Hengill earthquakes. All these are preceded by an increased seismic activity in their epicentral areas and with high SWSC values the last day before the earthquakes.

8 EARTHQUAKE WARNING ALGORITHM (EQWA) AND FALSE ALARM RATES

Based on the previous examples two different EQWA were designed and tested, one for the Hengill area and one for the SIL area. The following requirements were used:

- The FRMM value must exceed 150 m within a distance of 6 km and within a time period of one day (Hengill) or 130 days (SIL area) before the time of the warning.
- The SWSC value must exceed 50.0 within a distance of 6 km and within one day of the warning (Hengill).
- The "sandwich" ratio Q must exceed 0.65 within 6 km and within one day of the warning, in addition the number of events in the central strip must exceed 12 (a time window of 21 days) (SIL area).

Thus both in Hengill and SIL the FRMM is used, but in SIL area only as an intermediate–term precursor while in Hengill it is used as a short–term precursor. One must remember that the seismicity rate is almost two size orders higher in the Hengill area than in the SIL area. More information can be collected within a short–time interval.
The requirements above have been chosen so that all the earthquakes with $M_L \geq 4.9$ will be preceded by correct warnings. A warning is defined to be correct if it is followed by such an earthquake within 6 km and within 24 hours.
Figure 12 shows all warnings for the nine years 1991–2000. The 5 largest earthquakes are also shown. A large number of the warnings especially within the SIL area are caused by the high aftershock activity. This is natural as the "sandwich" Q–value is used there. What is more interesting (and shown in the Figures 13–17) is that also most of the warnings before the earthquakes are at places of future earthquakes. This is in agreement with other precursor studies in other parts of the world.

9 CONCLUSIONS

The following conclusions are made:

- The foreshock and microearthquake activity before large earthquakes within SW–Iceland do show variations in agreement with reports from other parts in the world.
- The foreshock activity can be used to indicate place and time of 500 times increased earthquake probability.
- Most false alarms are at "correct" places but are just coming too early (days, months, years).
- The results are in agreement with other studies of crustal strike–slip earthquakes both in precursor times, in distances involved, in foreshock magnitudes and frequencies, and in locations of false alarms.
- The monitoring of small microearthquakes (down to negative magnitudes) is essential in this study, the 20–30 microearthquakes giving the "sandwich" Q–value before the largest earthquake are mostly in the magnitude range –0.2 to 0.4 (M_L).
- The modified median of the fault radii (FRMM) shows a number of remarkable features and seems to be highly connected to the geodynamical processes (also over great distances).

10 DISCUSSION

The purpose of this study was to investigate the value of foreshocks for an EQWA within SW–Iceland. The basic idea behind the Icelandic seismometer network is to make full use of all detected microearthquakes. Due to low urban noise and lack of thick sediments a resonably dense network (spacing of 20 km in SW–Iceland) can detect and analyze microearthquakes down to negative magnitudes. This means that this foreshock activity study has better possibilities than studies where only fairly strong foreshocks (magnitudes larger than 1 or often 2) are included.

As mentioned the increase in the probability to have an earthquake during an alarm is of the order of a factor 500 compared to randomness. It is obvious that with knowledge of such a high increase it would be irresponsible not to inform those possibly affected.

As most of the false alarms tend to be at the "right" places it is likely that the false alarms also will increase the earthquake security in the area (less number of heavy items placed high and not fixed, etc.) as probably many persons taking precautions will not undo them after the 24 hours of warning.

This study is retrospective and does not show that the future earthquakes will be similar to those studied here. A very interesting result of this study is that everything we have observed is in excellent agreement with previous observations of other crustal strike–slip earthquakes at other places in the world. The times involved, the distances involved, and the earthquake sizes (main shocks and foreshocks) involved. This indicates that even if we cannot be sure it is likely that most of the future earthquakes in SW–Iceland will behave similar to those studied here.

As the precursor time is typically only a few hours it is necessary to rely on automatic microearthquake analysis for the short–term warnings.

Finally one should point out that the false alarm rate within SIL increased after the first large earthquake. In general one would expect that it may be more problematic to make warnings after a large earthquake as the seismicity is so much changed by the first large earthquake. Thus one probably has to make the algorithm adaptive to the changes in the seismicity. One way is to relate the thresholds adaptively to the rate of false alarms, another way may be to only point out the most likely place(s) if a new big earthquake would occur.

The EQWA presented here just shows an *a posteriori* study which actually includes parameters found to work for the earthquakes included. It shows, however, that there are several precursory phenomena (FRMM highs and increases, Q highs, SWSC highs) that can and probably should be included in more complete EQWA (earthquake warning algorithms).

11 REFERENCES

Boatwright, J. & M. Cocco 1996. Frictional constraints on crustal faulting. *J. Geophys. Res.* 101, 13895–13909.

Dieterich, J.H. 1972. Time–dependent friction as possible mechanism for aftershocks. *J. Geophys. Res.* 77, 3771–3781.

Dieterich, J.H. 1974. Earthquake mechanisms and modeling. *Annu. Rev. Earth Planet. Sci.* 2, 275–301.

Dieterich, J.H. 1978. Time–dependent friction and the mechanics of stick–slip. *Pure Appl. Geophys.* 116, 790–806.

Dieterich, J.H. 1979. Modeling of rock friction. 1. Experimental results and constitutive equations. *J. Geophys. Res.* 84, 2161–2168.

Dieterich, J.H. 1979. Modeling of rock friction. 2. Simulation of preseismic slip. *J. Geophys. Res.* 84, 2169–2175.

Dieterich, J.H. 1986. Earthquake source mechanisms. In: S. Das, J. Boatwright & Scholz (editors), *Geophys. Monogr. Series* 24, American Geophysical Union, Washington D.C., 37–49.

Dieterich, J.H. 1992. Earthquake nucleation on faults on rate– and state–dependent strength. *Tectonophysics* 211, 115–134.

Evison, F.F. 1977. The precursory earthquake swarm. *Phys. Earth Planet. Int.* 15, P19–P23.

Jones, L.M. 1984. Foreshocks (1966–1980) in the San Andreas system, California. *Bull. Seism. Soc. Am.* 74, 1361–1380.

Jones, L.M. & P. Molnar 1979. Some characteristics of foreshocks and their possible relationship to earthquake prediction and premonitory slip on faults. *J. Geophys. Res.* 84, 3596–3608.

Rikitake, T. 1975. Earthquake precursors. *Bull. Seism. Soc. Am.* 65, 1133–1162.

Roy, M. & C. Marone 1996. Earthquake nucleation on model faults with rate– and state–dependent friction: Effects of inertia. *J. Geophys. Res.* 101, 13919–13932.

Ruina, A. 1983. Slip instability and state variable friction laws. *J. Geophys. Res.* 88, 10359–10370.

Rögnvaldsson, S.Th. & R. Slunga 1993. Routine fault plane solutions for local networks: a test with synthetic data. *Bull. Seism. Soc. Am.* 83, 1232–1247.

Slunga, R. 1981. Earthquake source mechanism determination by use of body–wave amplitudes – an application to Swedish earthquakes. *Bull. Seism. Soc. Am.* 71, 25–35.

Slunga, R. 1982. Research on Swedish earthquakes 1980–1981. *FOA Report* C 20477–T1. Swedish National Defence Establishment, Stockholm, 189 pp.

Slunga, R. 1991. The Baltic shield earthquakes. *Tectonophysics* 189, 323–331.

Stefánsson, R., R. Böðvarsson, R. Slunga, P. Einarsson, S.S. Jakobsdóttir, H. Bungum, S. Gregersen, J. Havskov, J. Hjelme & H. Korhonen 1993. Earthquake prediction research in the South Iceland seismic zone and the SIL project. *Bull. Seism. Soc. Am.* 83, 696–716.

Tse, S.T. & J.R. Rice 1986. Crustal earthquake instabilty in relation to the depth variation of frictional slip properties. *J. Geophys. Res.* 91, 9452–9472.

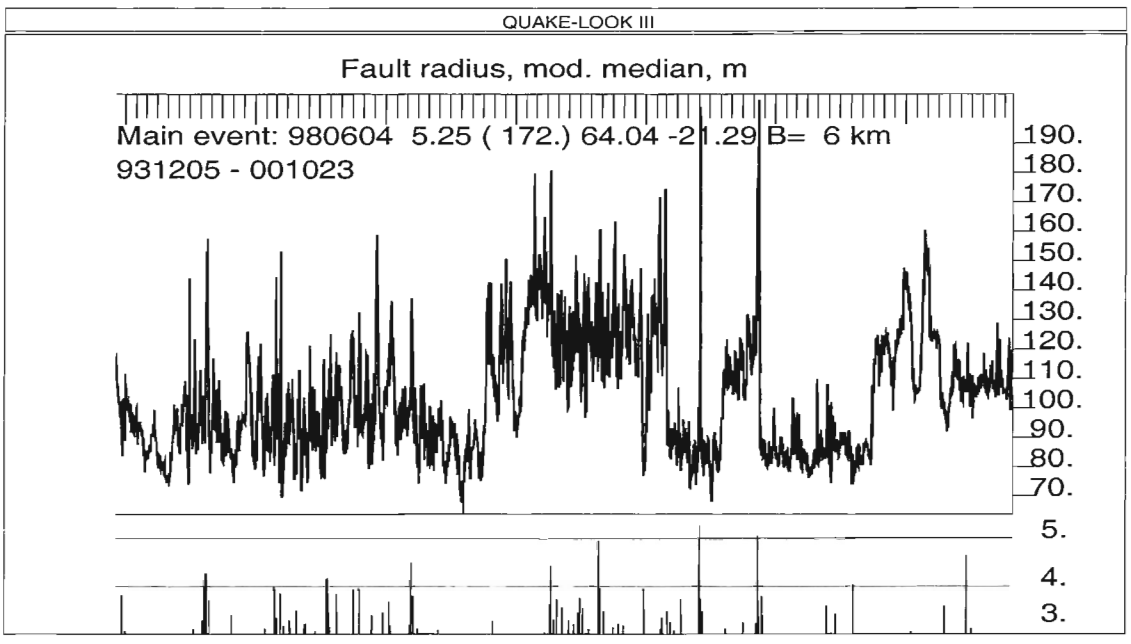

Figure 1. *The figure shows the FRMM in meters computed for times and places within a N–S strip between 63.9°N and 64.1°N and with a width of 6 km centered at longitude 21.29°W. At the bottom the earthquakes with $M_L \geq 3$ and within the strip are shown. One can see a very non–random behaviour of the fault radius. The general level is rather constant from July 1, 1991, up to October 1996 (the marks in the upper part shows months and years) when it starts to rise and stays at a high level. It is interesting that this coincides well with the huge eruption in the Vatnajökull volcano. This indicates that this eruption is associated with stress change also in the Hengill area far away from the volcano. This supports the theoretically based assumption that the fault radius will reflect changes in the geodynamic loading. One can note that the two highest values are close coinciding with the times of the two largest earthquakes of the Hengill area. One can also note that a large double peak (exceeding 170 m) occurs 3–4 months before the largest earthquake.*

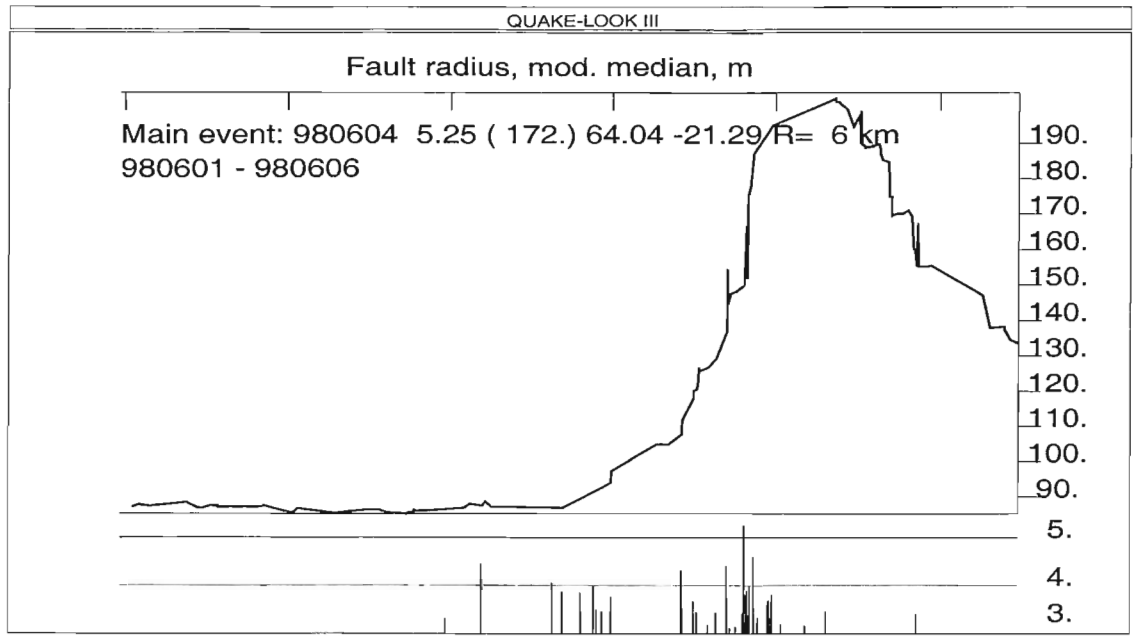

Figure 2. *This figure shows a part of Figure 1, the marks at the top show now days. Note the increase of FRMM during the last day prior to the major June 4, 1998, earthquake, the largest event mark at the bottom.*

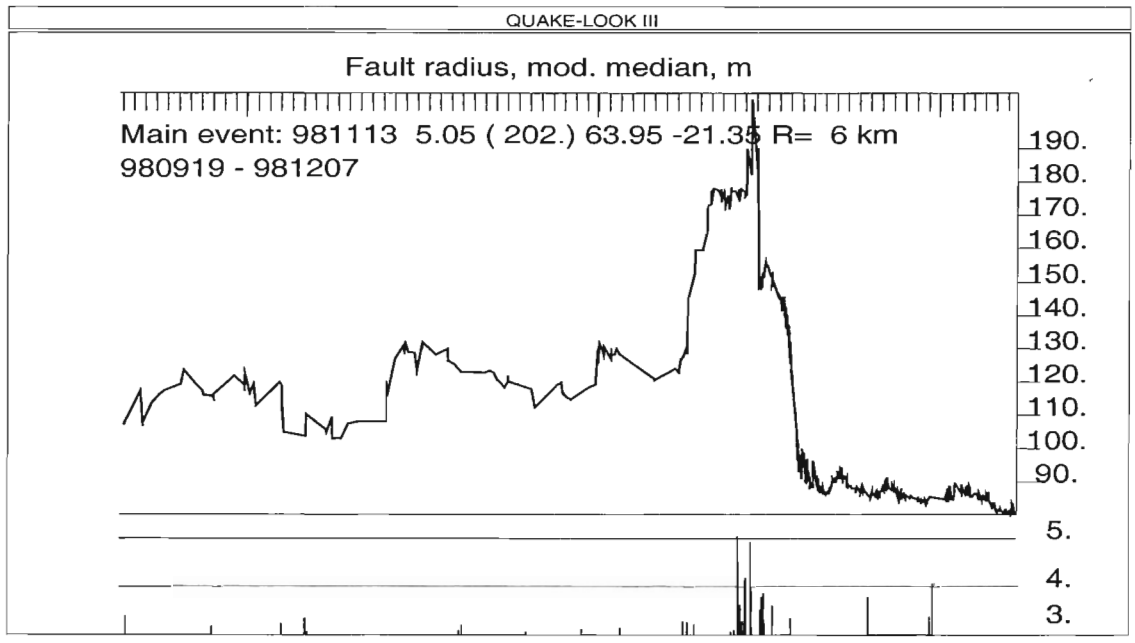

Figure 3. *This figure shows another part of Figure 1, now around the next largest earthquake within the Hengill area (the largest earthquake mark at the bottom). The time marks at the top show days and months. In this case the FRMM increases to a high value a few days before the earthquake and remains so until the main event. In Figure 1 one can see that after this earthquake the level drops dramatically to a very low level.*

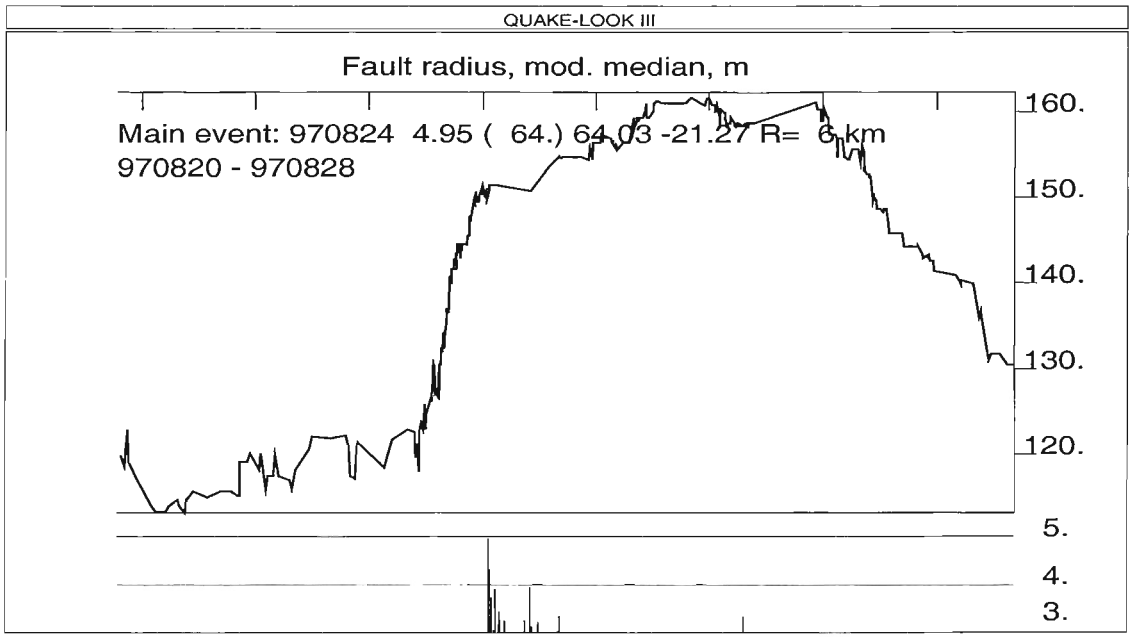

Figure 4. *This figure shows another part of Figure 1, now around the third largest earthquake within the Hengill area (the largest mark at the bottom). The time marks show now days. Again the increase of the FRMM starts during the last day prior to the earthquake and stays at a value over 150 m for a few days.*

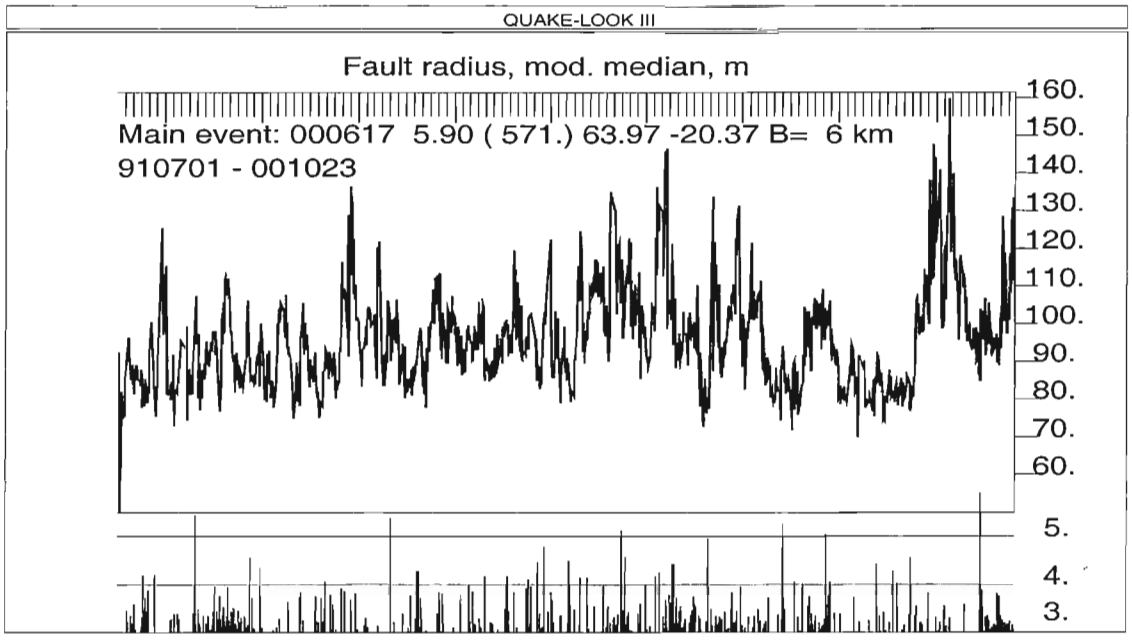

Figure 5. *This figure is similar to Figure 1 but now the strip is within the SIL area and centered around the longitude of the large June 17, 2000, earthquake. This event is shown by the largest event mark at the bottom. Now we see no large increase of the FRMM prior or coincident with this earthquake indicating a quite different behaviour compared to the Hengill area. Note, however, that the largest values (exceeding 150 m) occur about 4 months prior this earthquake. Note also that the Vatnajökull eruption is not evident by the FRMM values. Note, however, that several of the features of the Hengill area (Figure 1) are also evident within this area in SIL.*

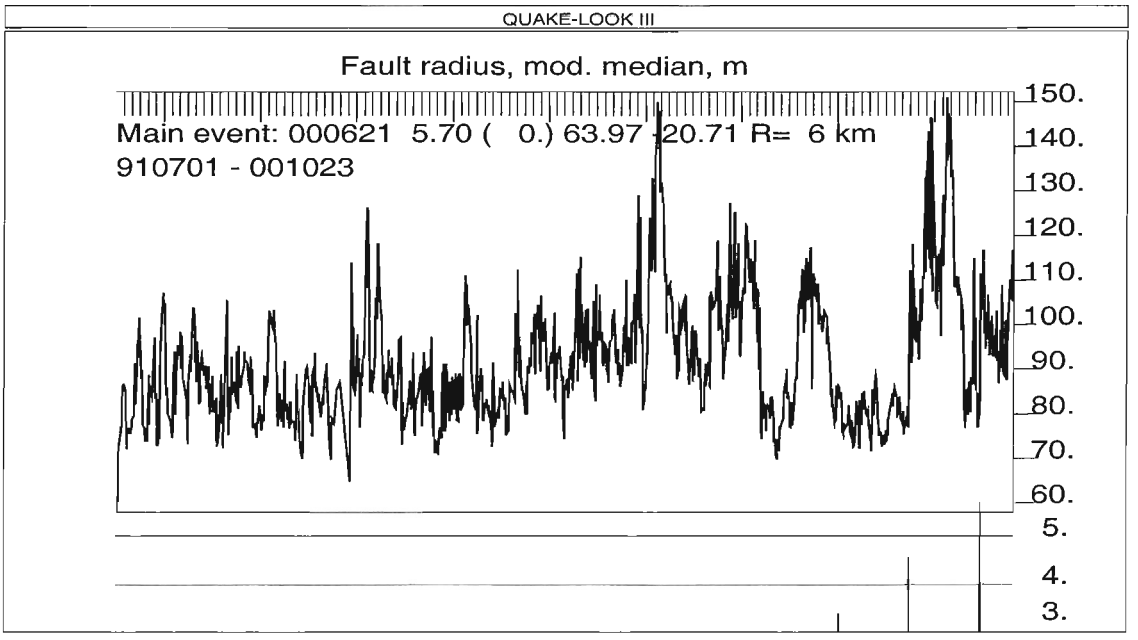

Figure 6. *This figure is similar to Figure 5 but now the strip is centered around the second large earthquake (June 21, 2000) within the SIL area. The earthquake is marked by the largest mark at the bottom. This time there is an increase of the FRMM the last days before the earthquake but not to a very high level. Again we see the largest value about 4 months before the earthquake. In this figure the events at the bottom are all within the strip. Note the sharp increase coinciding with the magnitude 4.5 earthquake.*

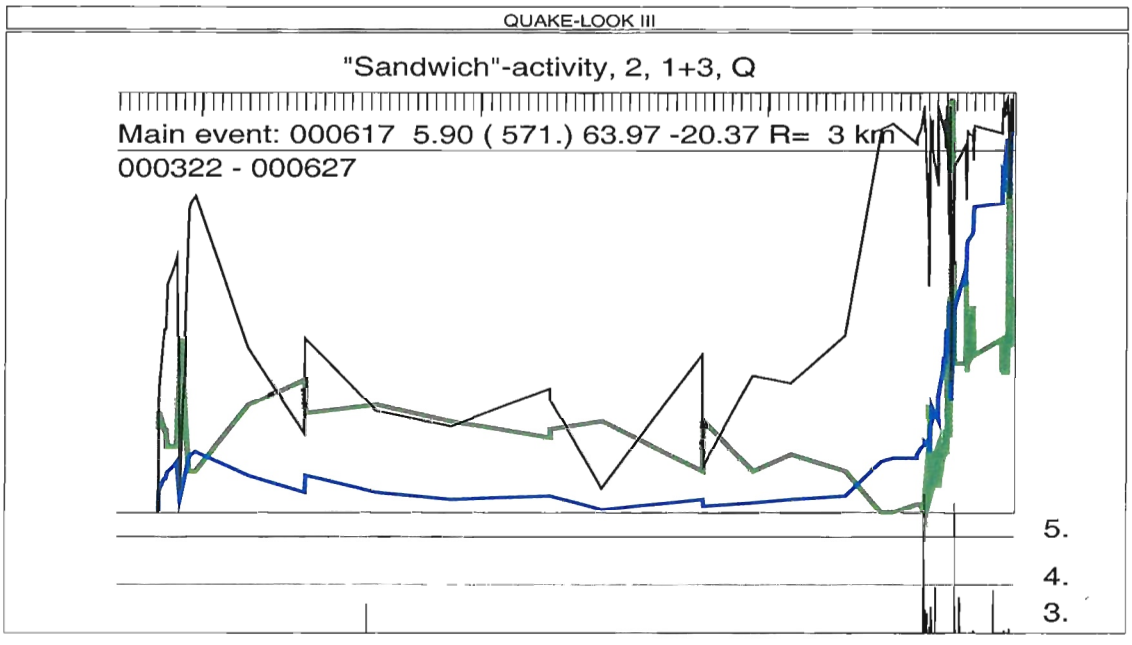

Figure 7. *This figure illustrates the "sandwich" seismicity before the June 17, 2000, large SIL earthquake. The time marks at the top show days and months. The thick black line increasing about a week before the earthquake (the largest mark at the bottom) is the seismicity within the central strip. The thick gray line decreasing before the earthquake is the seismicity within the surrounding strips. The thin black line is the ratio, Q, of the two previous parameters. The thin line shows Q=0.75. The time window used in computing these seismicity rates is 21 days. Thus the figure shows that the silence in the surroundings is lasting for about one month. The increase within the central strip is largest about a week before the event.*

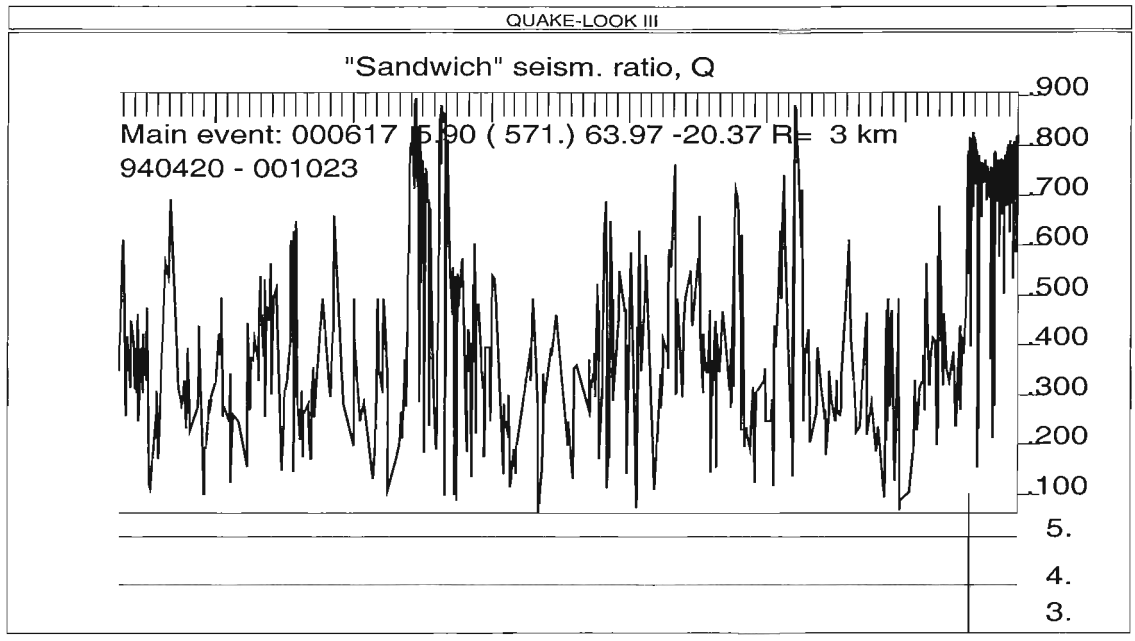

Figure 8. *This figure shows the behaviour of the Q prior to the June 17, 2000, earthquake computed for microearthquakes close to the epicenter. Note that there are only a few periods of high values.*

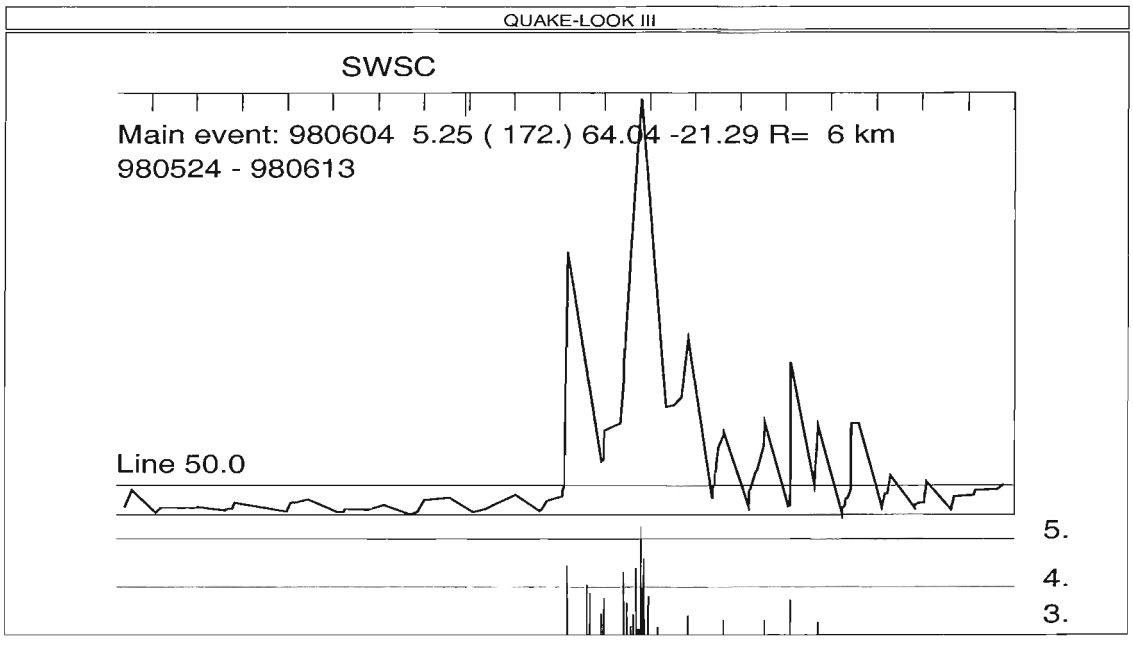

Figure 9. *The figure shows the behaviour of the slipweighted seismicity concentration before the largest Hengill earthquake. The time marks are days and the largest earthquake mark at the bottom is the June 4, 1998, earthquake. Note the extreme foreshock activity before this earthquake.*

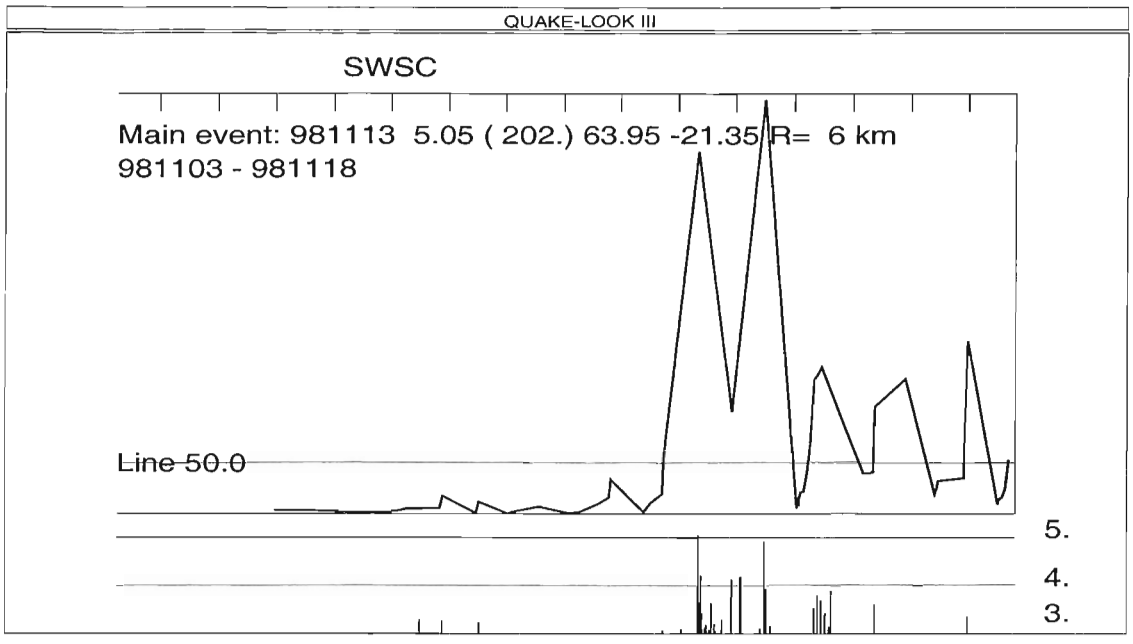

Figure 10. *The same as Figure 9 but before the next largest earthquake within the Hengill area, November 13, 1998.*

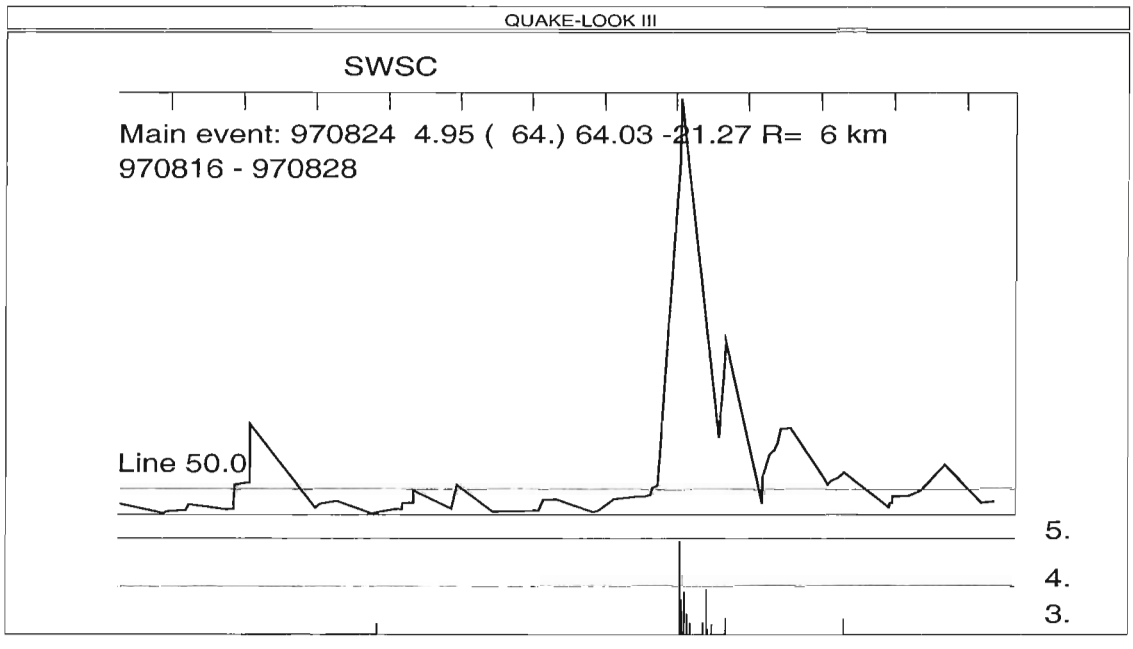

Figure 11. *As previous two figures but for the third largest Hengill earthquake, August 24, 1997.*

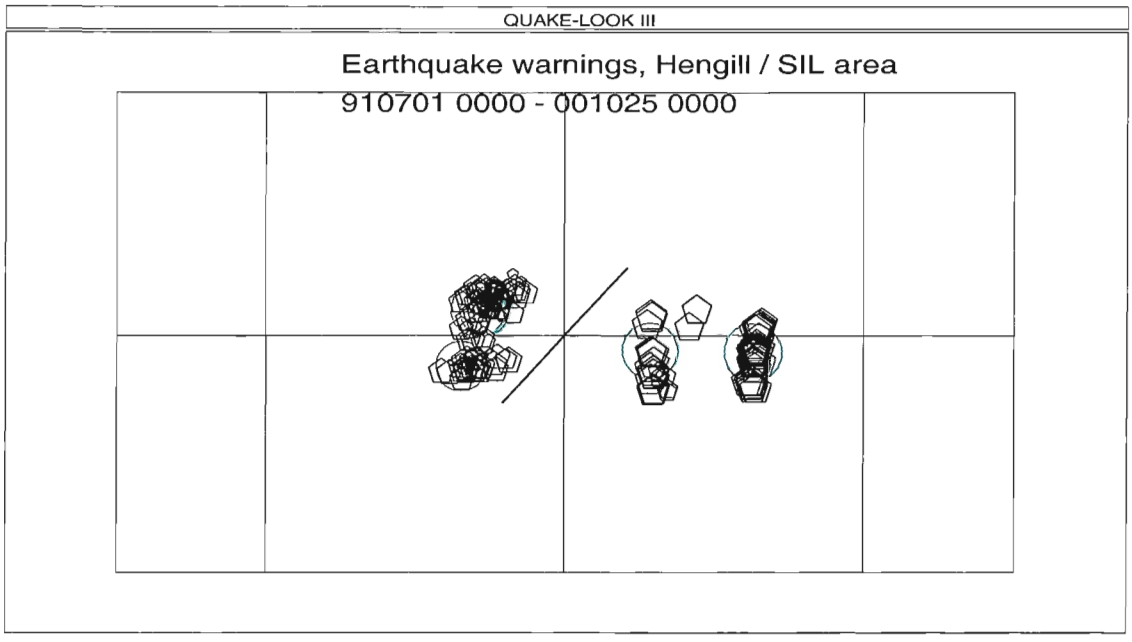

Figure 12. *The figure shows the warnings achieved by the EQWA as described in the text. The horizontal line marks latitude 64°N and the vertical lines mark longitudes 22°W, 21°W, and 20°W. The distance between the longitudes is about 49 km. The warnings are marked by pentagons. The warnings are scaled according to the time, all are within the time period and they increase in size with time. The circles mark the 5 largest earthquakes. The border line between Hengill and SIL goes through 64°N and 21°W with an azimuth of N45°E. The area of the map east of this line is the SIL area where the two largest earthquakes took place. It is obvious that most of the alarms are at correct places but at wrong times which is illustrated by the following figures.*

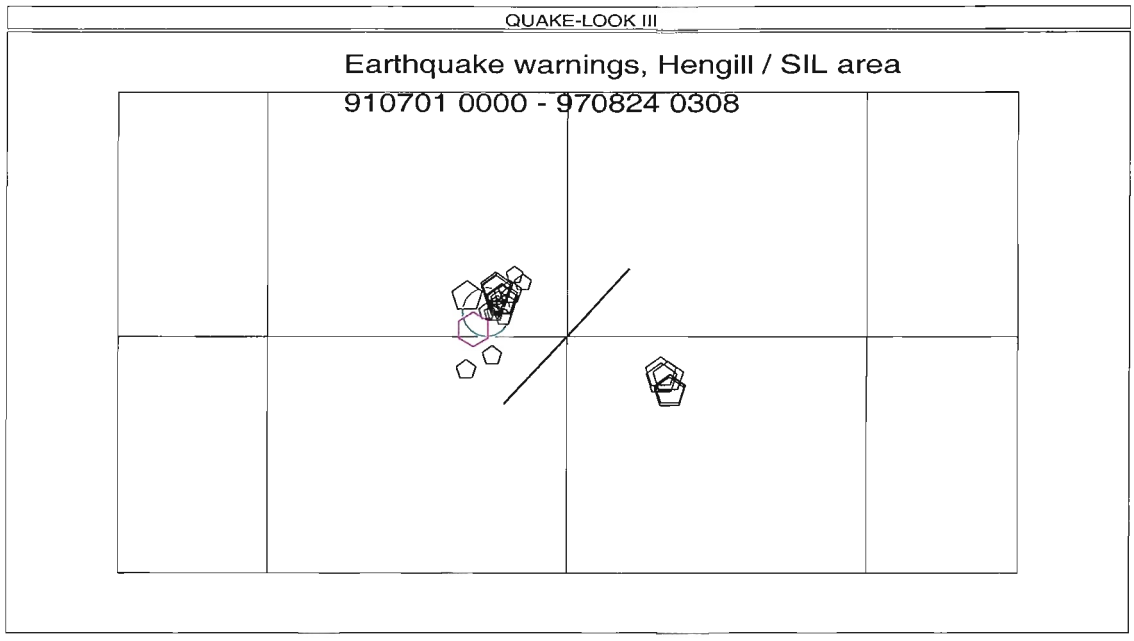

Figure 13. *The figure shows the 6 years before the earthquake on August 24, 1997. The warnings are shown as pentagons or hexagons (if they are less than 24 hours before the earthquake). We see that we have a number of too early warnings at correct or almost correct place plus a few warnings within SIL at the site of the future June 21, 2000, earthquake.*

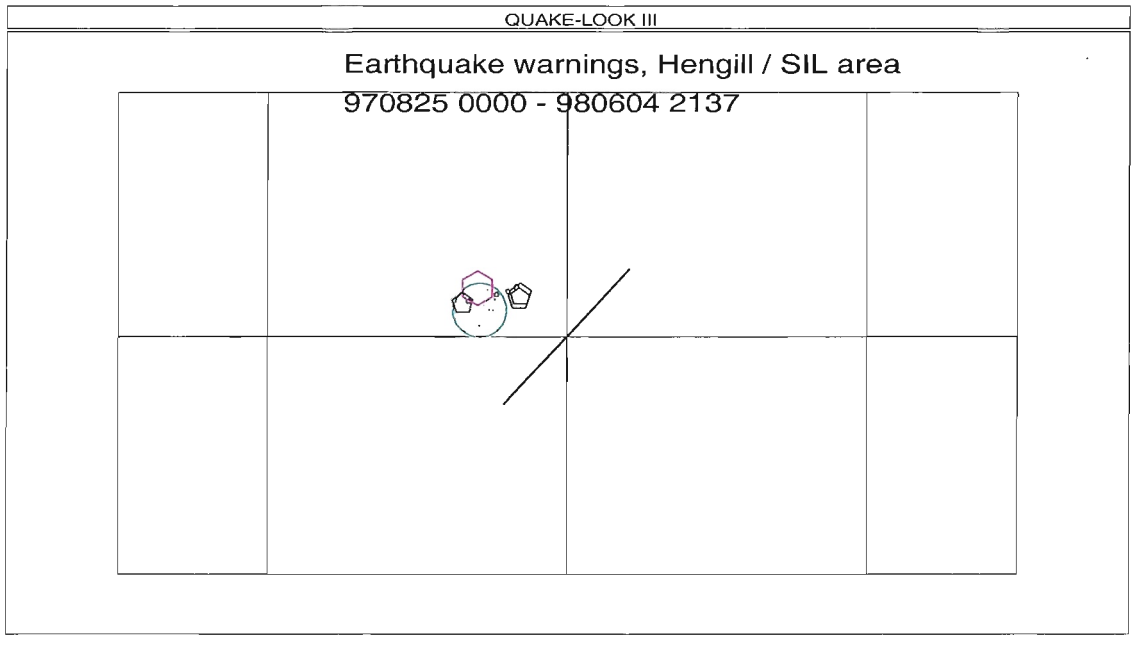

Figure 14. *The figure shows the warnings for the period after the August 24, 1997, event until the largest earthquake within the Hengill area, the June 4, 1998, earthquake. The warnings are scaled according to time, the very small marks are just in the beginning of the interval and are caused by the aftershocks of the previous earthquake. All warnings within this time interval are close to the coming earthquake.*

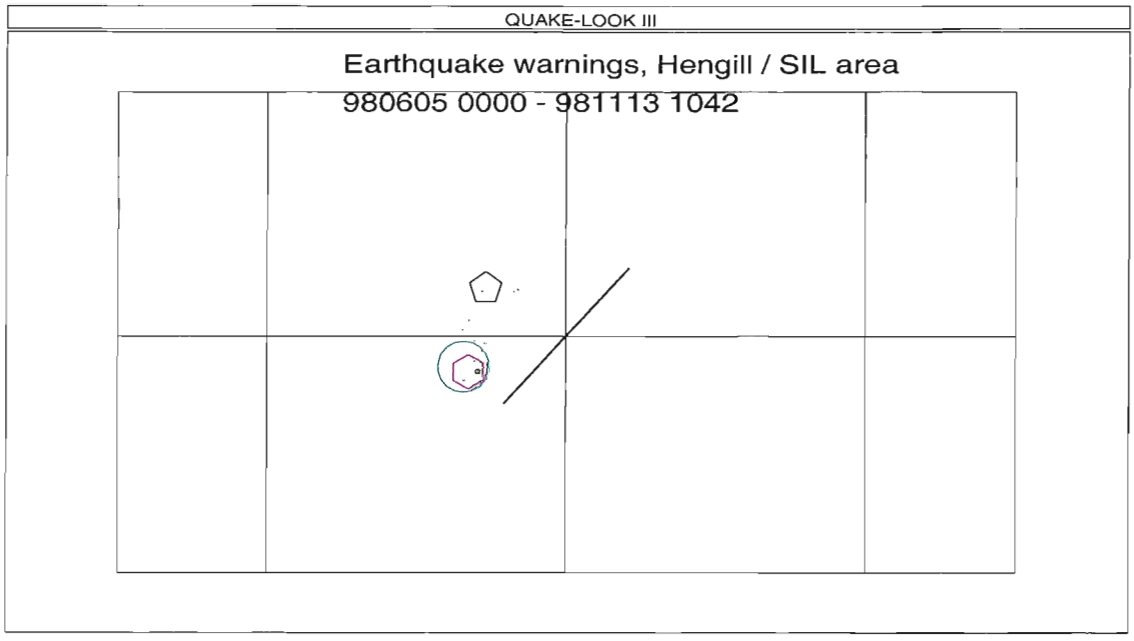

Figure 15. *This figure shows the warnings after the June 4, 1998, earthquake until the November 13, 1998, earthquake. Again the very small marks pertain to the very beginning of the time interval and are along the fault of the large earthquake. One of the two late warnings is close to the previous epicenter while the correctly timed warning also is at correct place.*

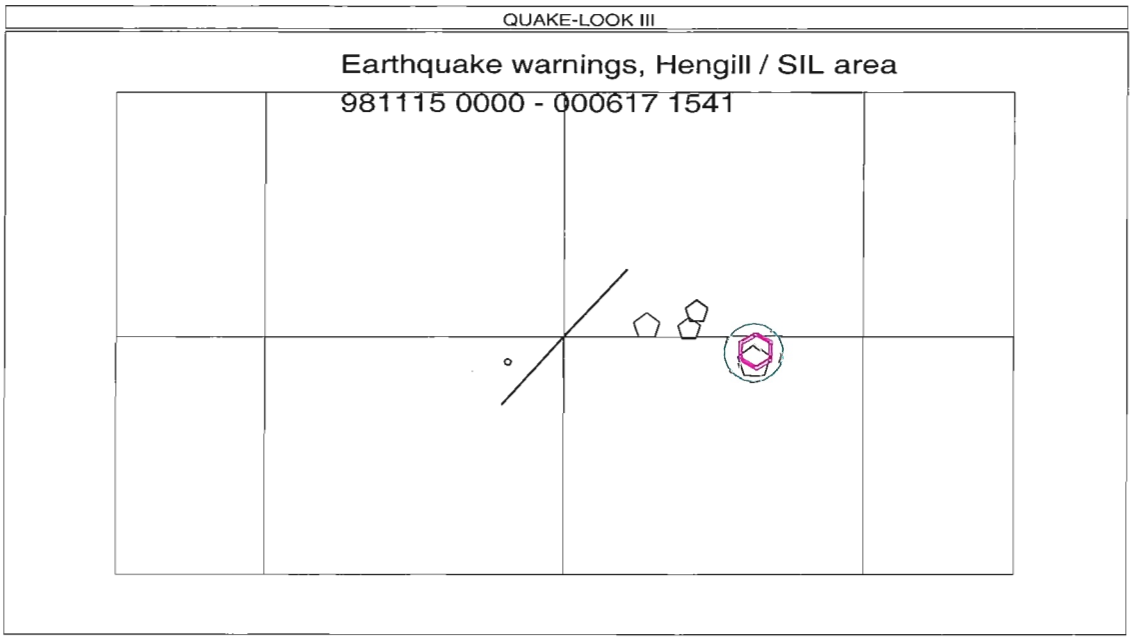

Figure 16. *This figure shows the warnings before the largest earthquake, June 17, 2000. Note that this time most of the warnings are within the SIL area. Of the three warnings in the SIL area which are at wrong place one is at the fault of the June 17, 2000, event. All the late warnings are at correct place.*

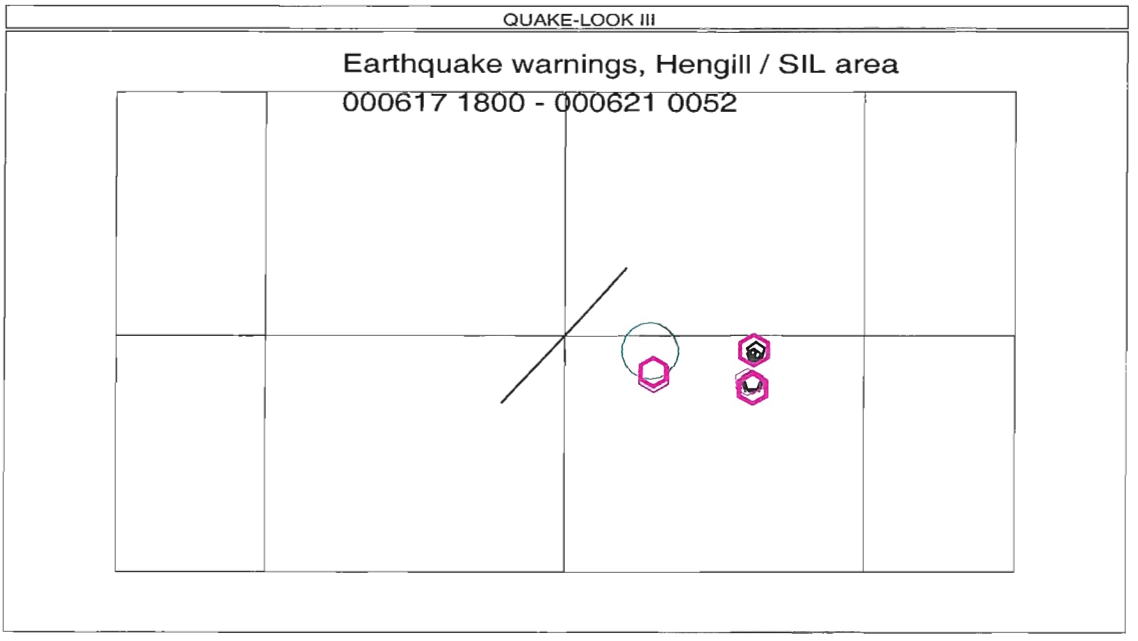

Figure 17. *The figure shows the short interval between the two large SIL earthquakes. This period had a very high activity, note however that all warnings at the correct place also are within 24 hours of the coming earthquake (and therefore marked as hexagons).*

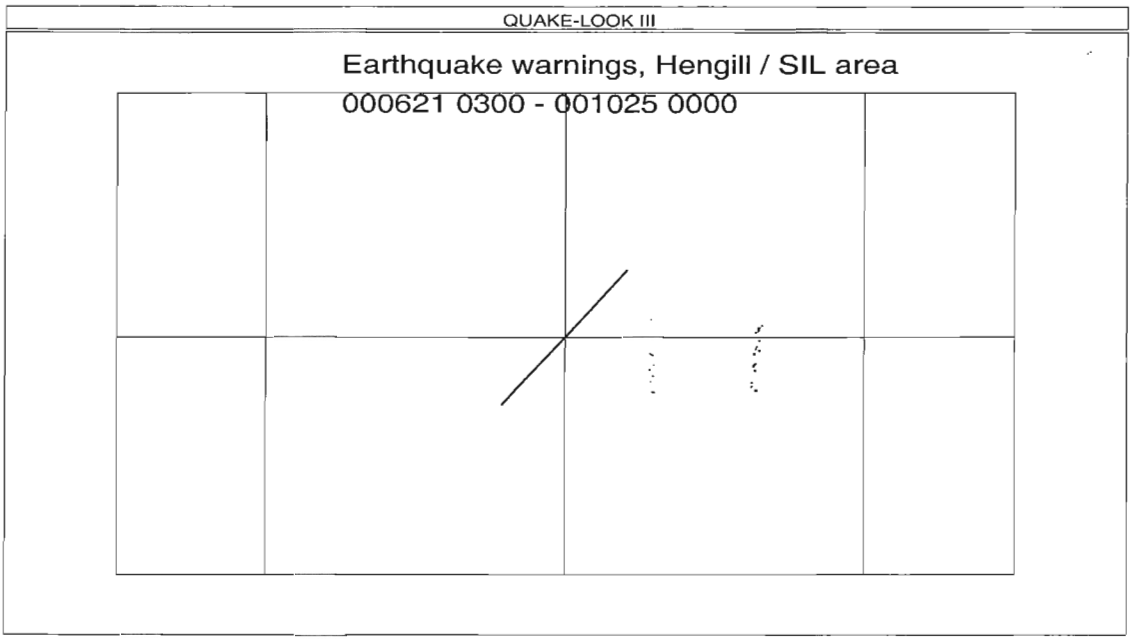

Figure 18. *This figure shows the time period after the last large SIL earthquake. Note again that there is no warning outside the SIL area and all warnings within SIL are along the faults of the two large earthquakes. The reason that the warnings stop already in July is due to lacking high FRMM values.*